

# Connection between the large-scale 500 hPa geopotential height fields and precipitation over Greece during wintertime

E. Xoplaki<sup>1,2,\*</sup>, J. Luterbacher<sup>1</sup>, R. Burkard<sup>1</sup>, I. Patrikas<sup>3</sup>, P. Maheras<sup>2</sup>

<sup>1</sup>Institute of Geography, University of Bern, Hallerstrasse 12, 3012 Bern, Switzerland

<sup>2</sup>Department of Meteorology and Climatology and <sup>3</sup>Division of Hydraulics, Faculty of Technology, University of Thessaloniki, 54006 Thessaloniki, Greece

**ABSTRACT:** The spatial distribution of the winter (December to February) precipitation over Greece was related to the eastern North Atlantic-European scale mid-tropospheric circulation fields by means of empirical orthogonal functions (EOFs) and canonical correlation analysis (CCA). The data used in this study are winter precipitation totals, of 23 stations, equally distributed over Greece, and winter mean 500 hPa geopotential heights (30 to 70° N, 30° W to 50° E) for the period 1958 to 1994. The Greek precipitation data were found to be homogeneous (Alexandersson test). A decrease of winter precipitation over the whole country was found, although significant (Mann-Kendall trend test) only over the northern and eastern parts and in the western mountainous regions. Three CCA patterns represent links that are very reasonable from a physical point of view. It is supposed that stronger westerlies over the eastern North Atlantic and the raising of the 500 hPa geopotential height (and also the sea level pressure) over continental Europe during the last few decades were connected with enhanced atmospheric stabilization and anomalous advection of cold and dry air from northerly directions. This led to the winter dryness over the eastern Mediterranean. The probable mechanisms and processes in the complex atmosphere-ocean system, leading to the regional anomalous climatic conditions, are discussed.

**KEY WORDS:** Greece · Winter precipitation · 500 hPa geopotential height · Empirical orthogonal functions (EOFs) · Canonical correlation analysis (CCA) · Atmospheric circulation

## 1. INTRODUCTION

Precipitation is one of the key parameters characterizing the regional climate of Greece. High-frequency (seasonal, annual, interannual) as well as low-frequency variations (e.g., interdecadal) of precipitation also play an important role in the management of regional agriculture, water resources, ecosystems, environment and economics in Greece. Identifying and understanding the influence of the large-scale atmospheric circulation patterns which produce variations of precipitation on different time scales over Greece is therefore crucial and of great importance.

Schönwiese et al. (1994, 1998) reported a pronounced significant trend to drier winter climate in the eastern Mediterranean area, especially over Greece for the period 1961 to 1990. They found a decrease of mean winter precipitation of around 60 mm for the same period.

The main physical and physico-geographical factors controlling the spatial distribution of the climatic conditions over Greece are the atmospheric circulation, the latitude, the altitude and, generally, the orography, the Mediterranean sea surface temperature (SST) distribution, the land-sea interactions (distance from the sea) and smaller-scale processes. Each of the factors represents its own characteristic influence on the Greek climate (Lolis et al. 1999). However, Trenberth

\*E-mail: xoplaki@giub.unibe.ch

(1990) and Xu (1993) point to the fact that the atmospheric circulation is the main forcing factor for the regional variability of temperature, precipitation (occurrence, total and spatial distribution) and other climate variables.

The pressure systems that influence the Greek winter precipitation are the Icelandic Low (indirectly), the low-pressure systems originating from the Atlantic Ocean or the Mediterranean (cyclogenesis; Gulf of Genoa) moving NW–SE, W–E or SW–NE, the lows from the region of Cyprus (cyclogenesis and/or reinforcement of moving lows), which produce precipitation with the interaction of the orography of the eastern Greece (Maheras 1982b) and the Aegean Sea. Due to its subsynoptic scale, the Aegean cyclogenesis (Flocas & Karacostas 1996) has been frequently underestimated in recent studies (Alpert et al. 1990, Trigo et al. 1999). In addition, the cyclones that originate in north Africa, near the Atlas Mountains, move to the northeast directly towards the eastern Mediterranean (Alpert et al. 1990, Trigo et al. 1999), producing rain over the Greek mainland.

The frontal depressions that approach Greece, from January to April, are important rain producers, especially along the west coast of Greece and in the central Aegean Sea. In winter, depressions originating in the Atlantic near the Straits of Gibraltar and tracking northeastwards barely cross the Adriatic, and consequently high rainfall probabilities are limited to the islands and the coastal areas of the Ionian Sea, with some influence extending to Thessaly (central Greece). As these frontal depressions approach Greece from the west they cause southwest winds over the Ionian and Aegean Seas that force the maritime air (which has been stagnating there) eastwards. Precipitation probabilities decrease south of this mean track partly because of surface retardation and partly because the depressions are decaying rapidly by the time they reach Greece (Flocas & Giles 1991).

In the above mechanisms, the frontogenetic influence of the warm Aegean Sea should also be mentioned. The variability in winter cyclonic routes in the eastern Mediterranean may be found in the changing land-sea contrast associated with the complex topography of the region. This contrast affects the geographical area of maximum low-level baroclinicity yielding significant monthly variations (Alpert et al. 1990).

The Greek precipitation field shows sharp gradient between the western part of the Greek peninsula (mainland and western Crete) (precipitation is 2 to 4 times higher; see Fig. 3) and the other areas of Greece (Fotiadi et al. 1999). The higher precipitation totals are related to the stronger thermal effect of the higher SSTs, during the winter, in association with the complex topography of the region. The air masses moving

towards the east pass over the sea, they are humidified in their lower layers, and they become unstable or potentially unstable. The condensation of the water vapor gained is a result of the orographical forcing by the land and the mountains and heavy rainfall follows on the windward side (Metaxas 1978).

It is well known that the upper troposphere mainly forces cyclogenesis over the central and eastern Mediterranean. Synoptic studies have demonstrated that the associated surface low pressure and therefore the frontal activity are most likely to develop under the southeastern side of upper level troughs (Prezerakos & Flocas 1996, 1997). Wibig (1999) investigated the relationship of circulation patterns of the 500 hPa geopotential heights in the Euro-Atlantic sector to the precipitation distribution in Europe during the winter months. She found that precipitation in the central and eastern Mediterranean is mainly related to the Central European pattern (CE; Wibig 1999), the Scandinavian pattern (Scand; Barnston & Livezey 1987, Rogers 1990) and the Eurasian pattern (EU2; Barnston & Livezey 1987).

Linkages between the non-seasonal precipitation over the extended Mediterranean region and monthly mean 500 hPa geopotential height over Atlantic and Europe have been investigated by Corte-Real et al. (1995) based on a canonical correlation analysis (CCA). They found statistically significant coupled patterns, some of them showing the Mediterranean Oscillation (Conte et al. 1989), namely anomalies in the geopotential height fields over the central-eastern Mediterranean and anomalies with opposite sign over the western Mediterranean. These are connected to specific Mediterranean precipitation patterns. Kozuchowski et al. (1992) studied the connections between precipitation and 500 hPa geopotential height fields for Thessaloniki and Athens for the period 1951 to 1985. They point to the fact that in winter high precipitation is connected with an upper level trough over the central Mediterranean and an upper level ridge over Scandinavia. This is in agreement with recent studies of Xoplaki et al. (1999), who investigated the influence of large-scale atmospheric circulation on the seasonal precipitation variability in Thessaloniki for the period 1958 to 1997. According to these studies, for Athens and Thessaloniki southeasterly or easterly airflow is responsible for high precipitation totals during winter-time. In addition, the mid-tropospheric circulation alone can share around 60% of the precipitation variability.

The precipitation regime, the geographical distribution and the relationship of precipitation between various meteorological stations in the Greek area have already been studied by Maheras & Kolyva-Machera (1979), Papadopoulos (1993), Sakellariou et al. (1993),

Sahsamanoglou (1993), Repapis et al. (1993), Lycoudis et al. (1994) and Fotiadi et al. (1999). Many climatologists have studied the relations between precipitation and multi-scale atmospheric circulation over Greece (Metaxas & Kallos 1980, Maheras 1982a,b, Maheras & Kolyva-Machera 1993, Metaxas et al. 1993, Rizou & Karacostas 1993, Luterbacher et al. 1998, Xoplaki et al. 1998, 1999). Most of these presentations of the observed climate variability or its connections with the Greek area focused on surface variables, i.e., temperature, precipitation and sea level pressure (SLP).

However, an extended study about the influence of the large-scale mid-tropospheric circulation in the production of low-frequency precipitation variations over Greece for the second half of this century is still lacking. In addition, the mechanisms and processes leading to long-term variations in the regional surface climate and upper level circulation are poorly understood so far.

The present study examines the characteristics of Greek winter precipitation and their relationship with the joint dominant modes of low-frequency atmospheric variability. The analysis focuses on wintertime (December, January and February), due to the importance of the precipitation totals for the Greek area during this season. The highest precipitation totals over Greece are observed during wintertime. In addition, the large-scale atmospheric circulation and the climate variables present a great spatial coherence during this season.

The concurrent relationship between winter precipitation in the Greek area and large-scale atmospheric circulation during the period 1958 to 1994 was investigated using empirical orthogonal functions (EOFs) in

combination with CCA. The results will be put in a wider time-space context and the probable mechanisms and processes in the complex atmosphere-ocean system leading to the regional anomalous climatic conditions (general decrease of winter precipitation) will be briefly discussed.

## 2. DATA

Two main data sets were used in this study: the time series of 6-hourly 500 hPa geopotential heights fields during the winter season and monthly winter precipitation for 23 Greek stations (Fig. 1b, including the altitude in m). All data sets cover the 1958 to 1994 interval.

The 6-hourly 500 hPa geopotential height fields are a product of the NCEP/NCAR 40-Year Reanalysis Project (Kalnay et al. 1996). The 500 hPa geopotential height data are given on a  $2.5^\circ \times 2.5^\circ$  latitude by longitude grid and the monthly mean values were computed from the 6-hourly fields. Because the surface climate is often sensitive to minor shifts in large-scale atmospheric patterns (e.g., Yarnal & Diaz 1986), in order to isolate the characteristics of atmospheric variability specified to the Greek area, a relatively small spatial window was selected. 561 grid points were considered, extending from  $30^\circ$  W to  $50^\circ$  E and  $30^\circ$  to  $70^\circ$  N (Fig. 1a). For the sake of compatibility with other climatological studies, the 3 common winter months (December, January and February [DJF]) were used. The precipitation data of the Greek stations of the National Meteorological Service stem from the Monthly Meteorological Bulletin (1958 to 1987) and the Statistical Bulletin of Greece (1988 to 1994).

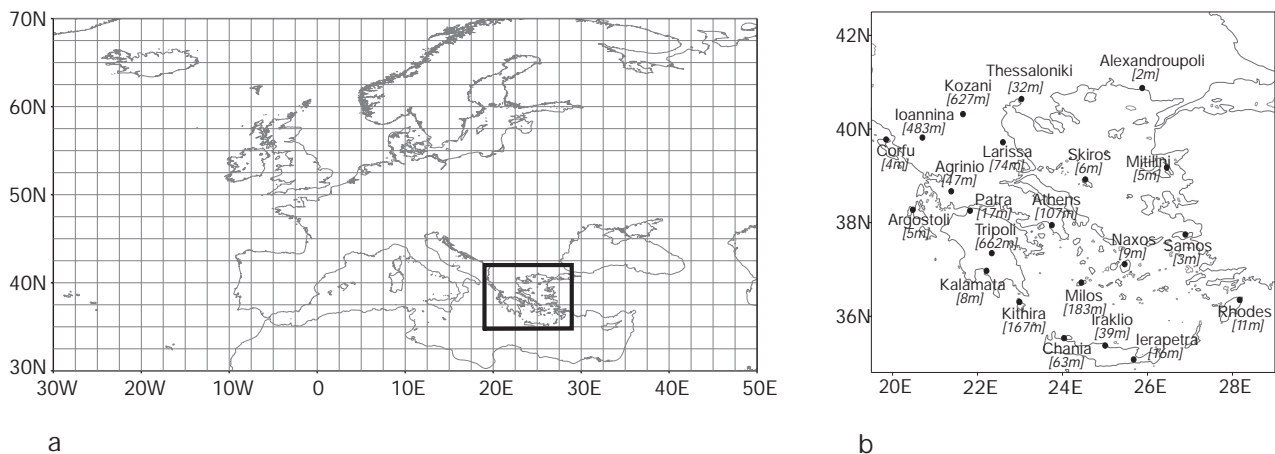


Fig. 1. (a) Distribution of the 561 grid points ( $2.5^\circ$  longitude by  $2.5^\circ$  latitude) with monthly mean 500 hPa geopotential heights representing the large-scale mid-tropospheric circulation. The area of Greece enclosed by the rectangular box is shown in additional detail in (b). (b) Geographical distribution of the 23 Greek stations. Stations' altitudes (m) are also given in brackets

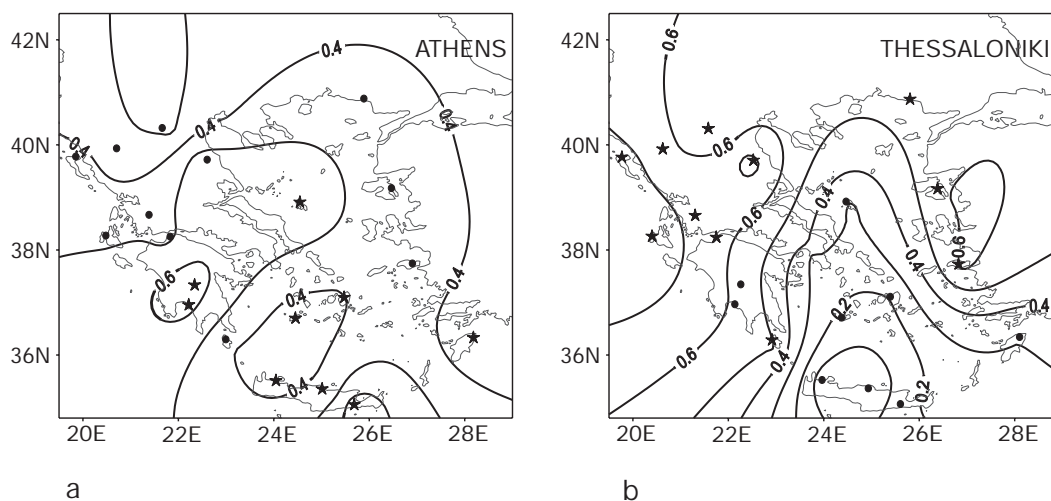


Fig. 2. Spatial correlation of winter precipitation between the reference series (a) Athens and (b) Thessaloniki and the remaining Greek stations. (★) Stations tested for homogeneity with the respective reference series

### 3. METHODS

The homogeneity of the precipitation data was tested using the Alexandersson (1986) test. The stations used as reference precipitation series were Athens and Thessaloniki. These 2 stations were selected because of their homogeneity, and are considered as highly homogeneous by all Greek researchers because there have been no changes in instruments, observing practices, the formulae for calculating means and the station environment (Peterson et al. 1998). Moreover, they show significant correlation with the tested time series and both stations have functioned continuously at the same location since their establishment. Fig. 2 presents the spatial correlation of winter precipitation between the reference series, Athens (Fig. 2a) and Thessaloniki (Fig. 2b), and the remaining Greek stations.

Athens shows higher correlations with the stations in the center and in the south, whereas the relationship between Thessaloniki and the stations in the west, north and east is closer than for Athens. All time series contained no missing values and were tested for homogeneity for every month and every season separately. Every station was tested with the reference time series (Athens or Thessaloniki) to which it showed the highest correlation. Stars in Fig. 2a,b indicate the stations used with Athens or Thessaloniki as the reference time series, respectively.

The linear trends for the winter precipitation for all Greek stations were calculated. The significance of these trends was tested by the non-parametric Mann-Kendall trend test (Sneyers 1992).

The 2 climatic data sets (500 hPa geopotential height fields and Greek station precipitation) were normal-

ized for each winter month, separately, by subtracting the respective 1958–1994 mean and dividing by the respective standard deviation. The 3 concatenated normalized winter months were then considered as 1 large vector and projected onto their first few EOFs. This procedure removes linear dependencies between variables within the same data set and reduces the dimensionality of the observed data. EOF analysis is a technique that is used to identify optimal representation of patterns (main signals), which maximizes the simultaneous variation (Preisendorfer 1988, von Storch 1995, von Storch & Zwiers 1999). In this study, the first 5 EOFs were retained for the winter 500 hPa geopotential height fields and the first 7 for the precipitation at the Greek stations; these numbers of EOFs share 80% of the total variance of the 500 hPa geopotential heights and precipitation, respectively. The EOF scores (time series) were used for the subsequent CCA (Barnett & Preisendorfer 1987, von Storch & Zwiers 1999). CCA determines optimal pairs of the concomitant spatial patterns that account for the maximum amount of variance within the gridded winter (DJF) 500 hPa geopotential heights and the Greek winter precipitation separately and, at the same time, their optimally correlated time components. The 2 temporal series (i.e., coefficient time series; 1 for each field) are the projections of the spatial patterns on the input data fields. The squared correlation between these temporal series is the maximized quantity and gives a measure of the degree of association between the 2 temporal patterns. The coefficient time series (i.e., the intensities of the modes) are normalized to unity, so that the canonical correlation patterns represent the typical strength of the signal, with the geopotential

height anomalies in geopotential meters (gpm) and the precipitation anomalies in mm.

To test the plausibility of the statistical relationships detected by means of CCA, 3 selected winters (1962/63, 1970/71 and 1991/92) were considered in more detail. The selected winters are characterized by negative time components, time components close to zero and positive time components of the first CCA pair, respectively.

For the transformation of the grid-point 500 hPa geopotential heights and Greek station-related information into a field analysis a 'kriging' interpolation scheme (Brown & Eischeid 1992) was used (except for Fig. 3b), where the contour lines give an 'optimum' between smoothing in space and realistic reproduction of the station data (Schönwiese et al. 1994). However, it has been taken into account that one cannot have high confidence in the interpolation of precipitation in regions where the station-to-station distances are large and where orography is an important factor (see below).

## 4. RESULTS

### 4.1. Homogeneity of the Greek precipitation data

The calculated Alexandersson test statistics,  $T_v$ , were at all stations lower than 4. The maximum value of  $T_v$ ,  $T_o$ , whether it exceeds a certain critical level or not, is used as a criterion of acceptance or rejection of the null hypothesis ( $H_0$ : inhomogeneity of the series). The critical levels, which naturally depend on the number of values in the series, for a 40 yr period are 7.0, 8.1 and 9.25 at the 90, 95 and 97.5% significance levels, respectively (Alexandersson 1986). This means

that all time series can be considered as rather homogeneous. Thus, no adjustment or corrections of the time series were made.

### 4.2. Mean Greek winter precipitation distribution and trend analysis

Fig. 3b reveals the distribution of mean winter precipitation in the period 1958 to 1994 together with the orographical conditions over Greece. It shows a maximum of precipitation in the western part of the country (mainly due to moist air advection from west and orographic uplift mechanisms due to the Pindos [NNW-SSE] chain and the mountains of Peloponnese [southern Greece]) up to 440 mm in the Ionian Sea. A minimum in winter precipitation is prevalent in the leeward rain shadow (central and northern Greece). A second maximum with values up to around 400 mm can be found over the eastern Greek islands mainly due to large-scale moisture advection in the low and mid-troposphere (including sensible and latent heat flux from the warmer Mediterranean Sea). The time series of winter mean precipitation at the 23 Greek stations exhibit small serial (winter-to-winter) correlation (not shown). Similar results have been found by Busuioc & von Storch (1996) for Romanian winter precipitation.

Since winter precipitation is related to the mid-tropospheric atmospheric circulation, Fig. 3a shows the winter mean 500 hPa geopotential heights, where an upper level ridge is located over the eastern North Atlantic towards western Europe and a small trough over eastern Europe.

In Fig. 4, the linear trends for the winter precipitation for 3 selected Greek stations are shown. Thessaloniki and Athens were used as they have the most homoge-

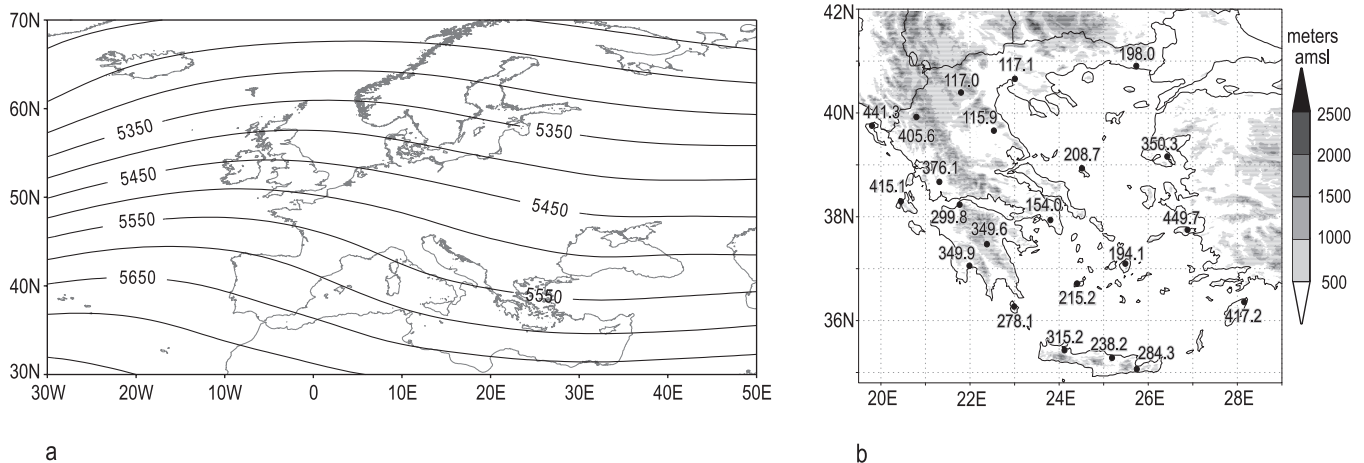


Fig. 3. (a) Seasonal mean of winter (DJF) 500 hPa geopotential heights (gpm). (b) Greek winter station precipitation (mm) for the period 1958 to 1994 together with the topography of Greece



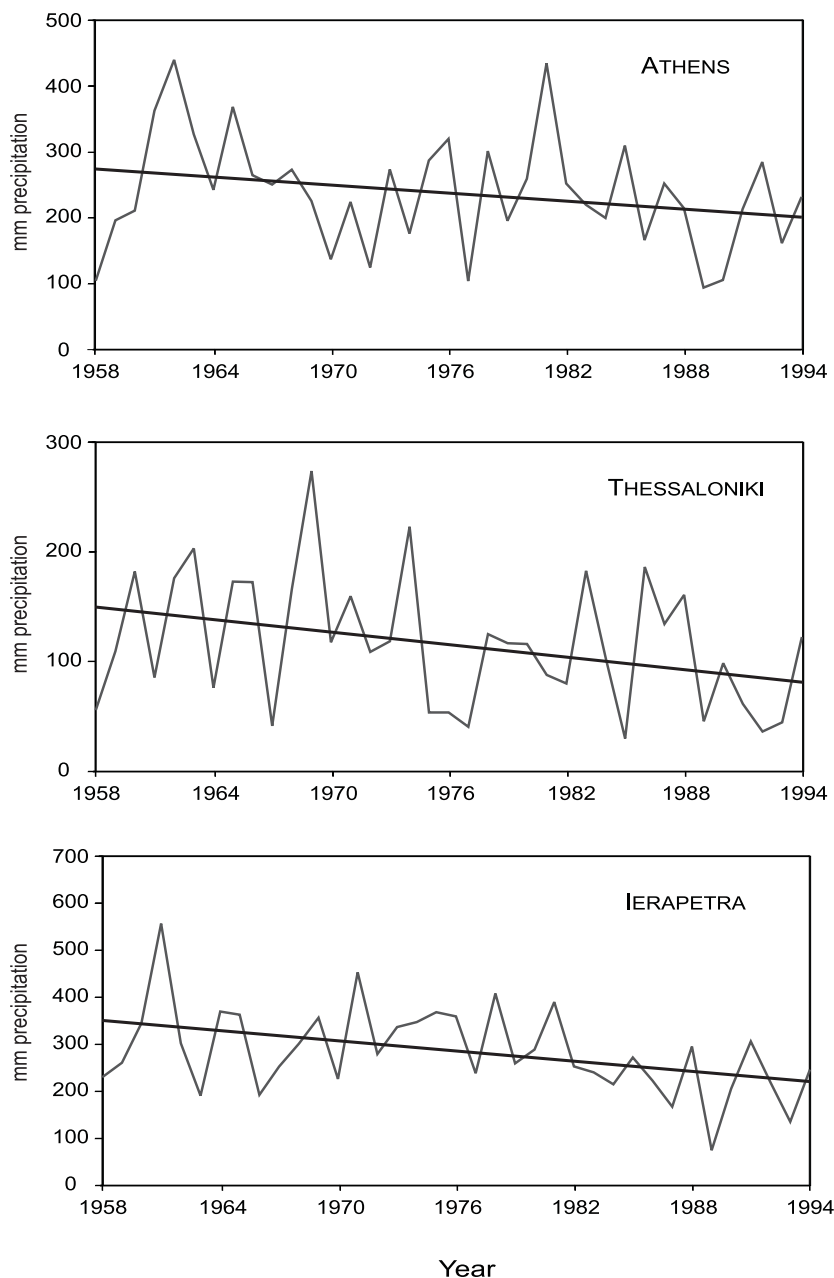


Fig. 4. Linear trend of winter precipitation for 3 selected Greek stations (Athens, Thessaloniki, Ierapetra). Note the different scales on precipitation axes

neous series and Ierapetra as a station representing the south Aegean Sea. The 3 time series indicate a decrease of winter total precipitation (Athens:  $1.8 \text{ mm winter}^{-1} \text{ yr}^{-1}$ ; Thessaloniki:  $1.7 \text{ mm winter}^{-1} \text{ yr}^{-1}$ ; Ierapetra:  $3.5 \text{ mm winter}^{-1} \text{ yr}^{-1}$ ). Fig. 5 reveals the Mann-Kendall trend test values for linear trends of Greek winter precipitation for the period 1958 to 1994. The 0.1 contour represents the 90% confidence level (error probability 0.1). The mountainous regions in the west (Ioannina, Agrinio, Patra and Tripoli), the Ionian

Islands (Corfu and Argostoli), over northern Greece (Thessaloniki) and the north and eastern Aegean region (Skyros, Mitilini, Samos and Rhodes) show a significant decrease of winter precipitation during the investigated period. All other stations show a decrease in winter precipitation as well, though not significant. The interpolated values based on the 'kriging' interpolation scheme (see above) over the western Ionian Sea, over the mountainous regions as well as over western Turkey are less certain, since no station data from

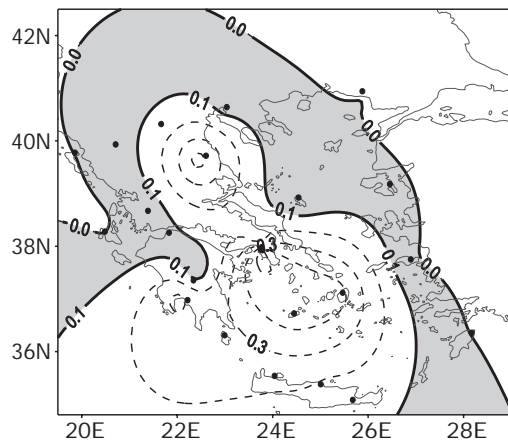


Fig. 5. Mann-Kendall trend test values for linear trends of Greek winter precipitation, 1958 to 1994. The 0.1 contour (thick solid line) represents the 90% confidence level (error probability 0.1). The shaded areas indicate a significant decrease of winter precipitation over the studied period

these areas were included in the study and, thus, should be considered with caution. This should be kept in mind for all the following maps.

#### 4.3. EOFs of Greek precipitation and large-scale 500 hPa geopotential height

To obtain insight into the main modes of variability of each parameter, Fig. 6 presents the first EOF (Fig. 6a) of the winter 500 hPa geopotential height and of the winter Greek precipitation (Fig. 6b) for the period 1958 to 1994. The leading EOF precipitation

pattern is characterized by a monopole pattern. This pattern explains 51% of the total variance of the precipitation field and describes the general mean winter precipitation structure (see Fig. 3b). It depicts simultaneous reduction (enhancement) of winter precipitation anomalies over Greece with 2 minima (maxima) up to 70 mm in the western part, in the Ionian Sea and over eastern Greece. Despite the complex topography of Greece, this large-scale pattern suggests a common physical process dominating the precipitation variability, which could be linked to large-scale atmospheric circulation. The leading 500 hPa geopotential height pattern explains around 25% of the variance and shows a dipole structure with positive (negative) geopotential height anomalies south of around 50° N and negative (positive) geopotential height anomalies over northern Europe. This mode portrays northward or southward migration of the storm tracks from their time-mean position, since the pair of extrema tends to straddle the climatological storm track axis (Lau 1988).

The second EOF precipitation pattern (Fig. 7b) accounts for 12% of variance and has a dipole structure, the negative and positive values being separated approximately by the coastline around the Aegean Sea. In addition, the highest precipitation anomalies are located over the Pindos chain (western part of Greece) and over Crete. Therefore, these patterns suggest a land-sea influence combined with orographic structures on winter Greek precipitation. This is in agreement with the studies by Kotinis-Zambakas et al. (1992) and Lolis et al. (1999), among others. The second EOF 500 hPa geopotential height pattern (Fig. 7a) explains around 20% of variance and shows a large anomaly with the same sign over almost the whole of continental Europe. A simultaneous rise (fall) of the

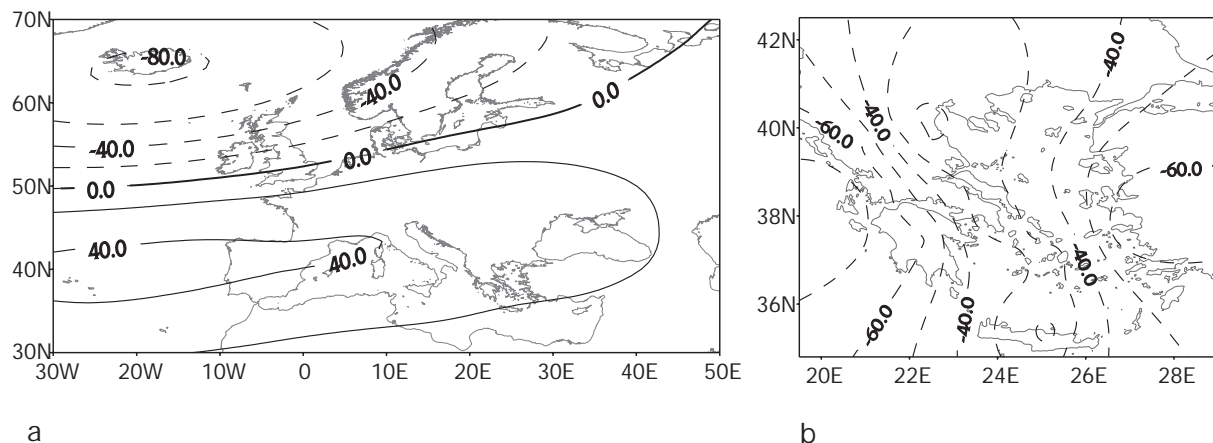


Fig. 6. Patterns of the first EOF of (a) the winter 500 hPa geopotential heights and (b) Greek winter precipitation (1958–1994). The coefficients are normalized to 1; therefore the patterns represent a typical dimensional distribution (gpm and mm). The explained variance is 25% (500 hPa geopotential height) and 51% (Greek precipitation)

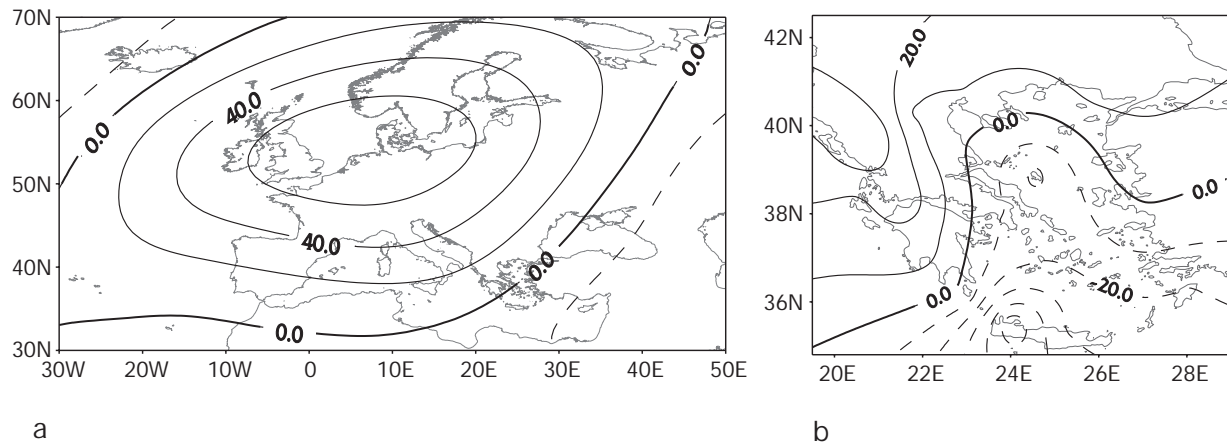


Fig. 7. Patterns of the second EOF of (a) the winter 500 hPa geopotential heights and (b) Greek winter precipitation (1958–1994). The coefficients are normalized to 1; therefore, the patterns represent a typical dimensional distribution (gpm and mm). The explained variance is 20% (500 hPa geopotential height) and 12% (Greek precipitation)

geopotential height is described by this pattern, with an amplitude of about 50 gpm over the North Sea. Greece is located at the southeastern edge of the monopole pattern.

The higher index precipitation and 500 hPa geopotential height patterns are more complex and they explain smaller amounts of variance.

#### 4.4 Coupled patterns between Greek winter precipitation and large-scale 500 hPa geopotential height fields

CCA yielded 3 physically reasonable relevant pairs of patterns that describe the simultaneous responses of the winter precipitation field to the anomalies of the mid-tropospheric circulation over the North Atlantic-European sector and therefore exhibiting circulation regimes concurrently associated with precipitation over Greece.

The first CCA pair (Fig. 8a,b) accounts for 17% of the total winter mean 500 hPa variance and for 38% of the total precipitation variability. This pair exhibits a correlation between the precipitation and the 500 hPa coefficient time series of 0.8. The precipitation pattern resembles the first EOF pattern, whereas the first CCA 500 hPa pattern is similar to the second EOF pattern. The mid-troposphere pattern resembles the Central European pattern (CE) (Wibig 1999).

According to this pattern, an intense, persistent and extended positive anomaly, centered over central Europe, is associated with below normal precipitation over the whole Greece. In the opposite phase, a remarkable anomalous upper level trough is connected with southwesterly moist air advection that

leads to rainy conditions, especially over western and eastern Greece. Minimum values are expected over the meridional Aegean Sea and the eastern part of Thessaly (central Greece) and central Macedonia (northern Greece). The year-to-year variations of the normalized time components of the first CCA pair are more or less coherent (Fig. 8c). The normalized time components of the 2 series (precipitation and 500 hPa geopotential heights) represent the corresponding 'sign' of the patterns shown in Fig. 8a,b. For instance, positive (negative) time components for both time series for a specific winter go along with positive (negative) anomalies of 500 hPa geopotential heights over Europe and negative (positive) precipitation anomalies over Greece. For both climate variables, the time components show a general downward tendency for more cyclonic situations in the mid-tropospheric fields for the first few years of the studied period. These are connected with wetter conditions over Greece. Positive normalized time components at the beginning of the 1970s and at the end of the studied period indicate blocking connected with drier conditions.

The second CCA pair (Fig. 9a,b) explains 16% of the total winter mean 500 hPa geopotential height variance and 14% of the total precipitation variability. The correlation between precipitation and 500 hPa geopotential height coefficient time series of the second CCA pair is 0.47. The precipitation pattern resembles the second EOF pattern, although the line between the positive and negative anomalies does not follow the border of the Aegean Sea. In the one mode (positive normalized time components), an anomalous high has its center over the Black Sea, while an anomalous upper level trough covers the eastern North Atlantic and large parts of Europe. Anomalous southwesterly



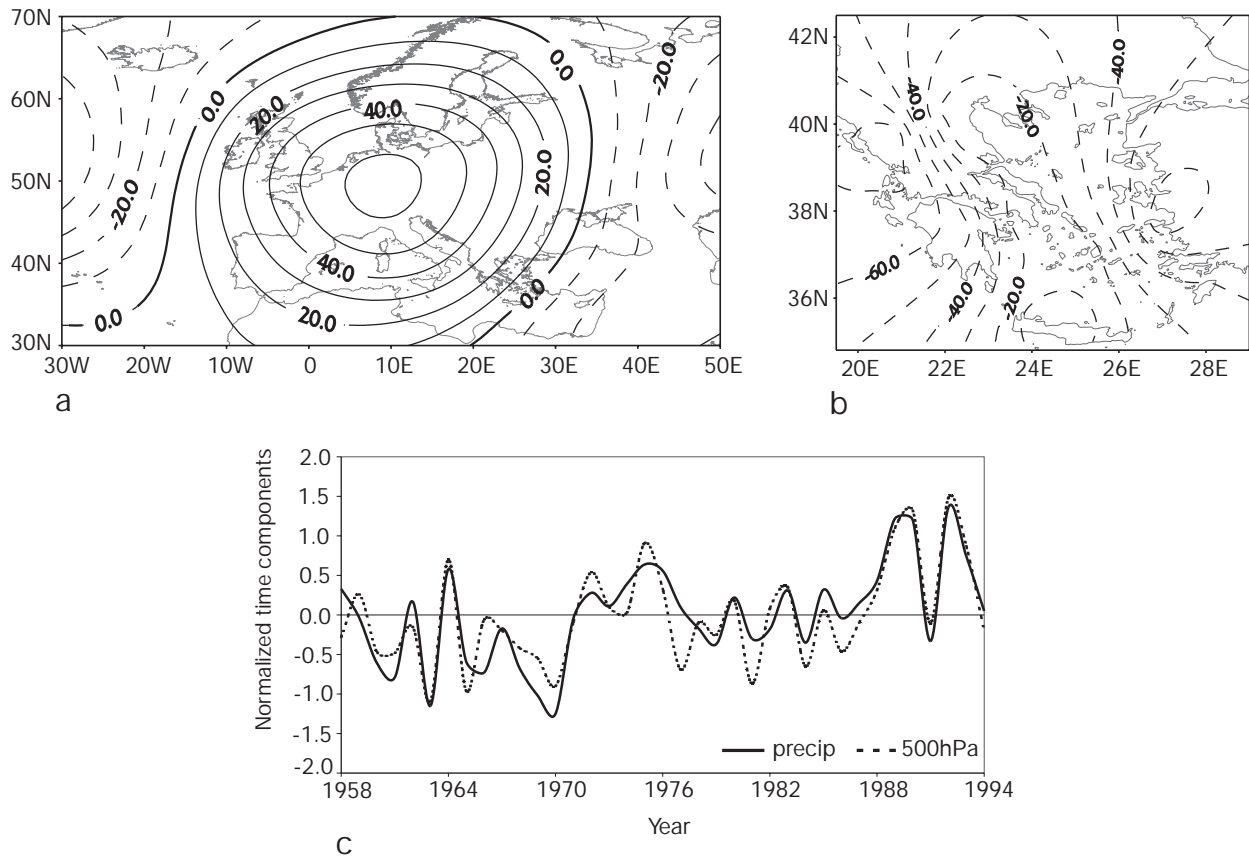


Fig. 8. Patterns of the first canonical pair of (a) winter 500 hPa geopotential height (anomalies in gpm; contour interval 10 gpm) and (b) total Greek winter precipitation (anomalies in mm; contour interval 10 mm). They explain 17% (500 hPa geopotential height) and 38% (Greek precipitation) of the total variance. Solid lines mark the positive values and dashed lines the negative values. (c) Normalized time components of the first CCA patterns of geopotential height anomalies (dashed line) and Greek precipitation anomalies (solid line). For clearness, the monthly (DJF) time components were averaged to 1 seasonal winter value for the respective years. The correlation between the 2 seasonal curves is 0.87

flow dominates over northern Greece. In the opposite phase (negative normalized time components), the upper level trough over eastern Europe leads to moist air advection, probably connected with enhanced instability and thus above-normal precipitation over the whole country, especially over the southern Aegean Sea. The year-to-year variations expressed by the time coefficients of the second CCA pair (Fig. 9c) are quite coherent, but they do not present a distinct trend during the whole period.

The third CCA pair (Fig. 10a,b) exhibits a correlation of 0.35 between the winter 500 hPa geopotential height and the Greek precipitation. It explains 13% of the total Greek winter precipitation variance and 17% of seasonal 500 hPa geopotential height variance. Persistent positive 500 hPa geopotential height anomalies are located over Scandinavia, central and northern Europe, while over the western Mediterranean negative anomalies are prevalent. Greece lies in the transi-

tion zone between the 2 upper level anomaly fields, where anomalous easterly to northeasterly (northwesterly) upper air currents effect the area. Analogously, opposite synoptic processes with reversed climate behavior take place in the other phase. The year-to-year variations in the winter normalized time components are high (Fig. 10c), with the positive mode prevailing during the early 1970s.

The fourth CCA pair (not shown) shows a smaller correlation of 0.31 and it is not of great relevance, since, in the case of Greek winter precipitation, less than 7% of variance is explained. Thus, this pattern describes only details at single stations. In the case of 500 hPa geopotential height the corresponding upper level pattern is still large scale and accounts for a considerable amount of variance (13%). It shows an extended positive anomaly over northwestern Europe and an extended belt of low 500 hPa geopotential heights from the Azores towards western Russia.

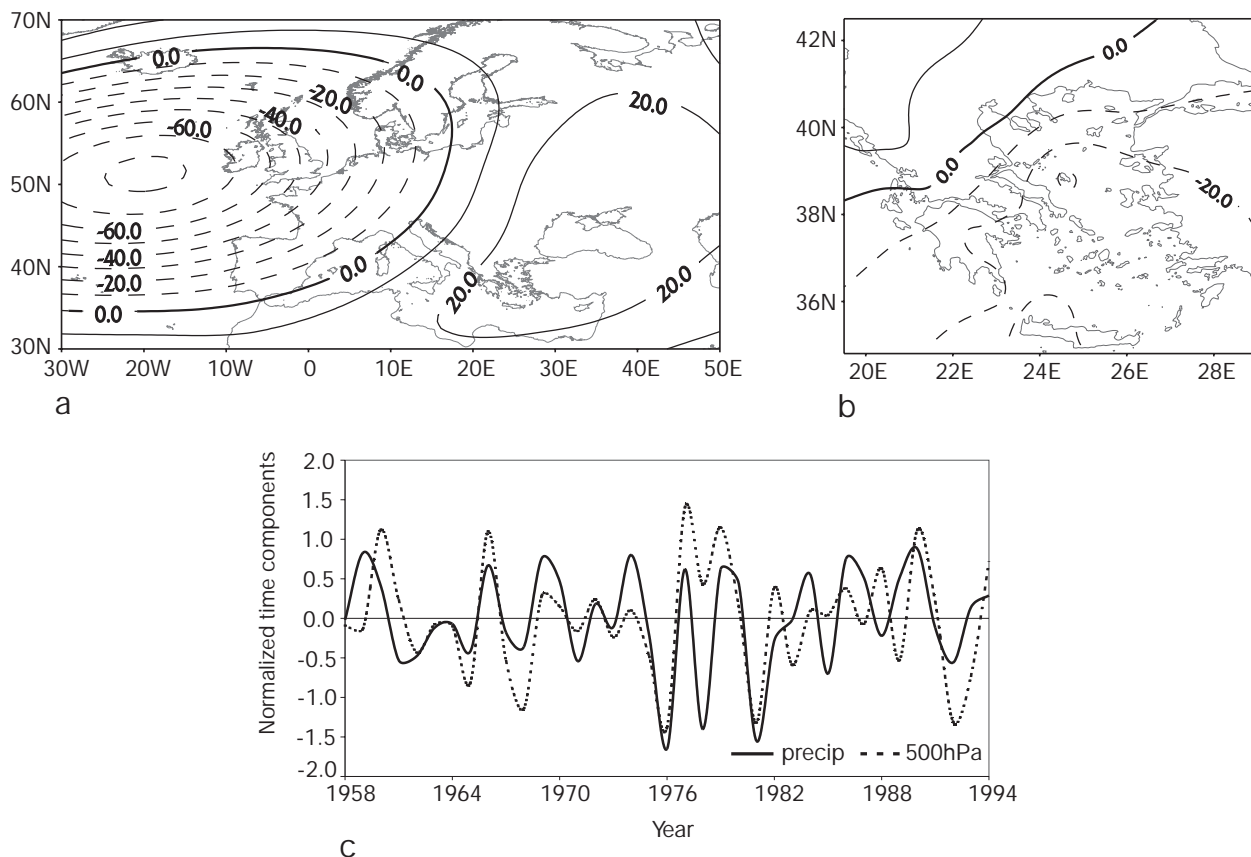


Fig. 9. Patterns of the second canonical pair of (a) winter 500 hPa geopotential height (anomalies in gpm; contour interval 10 gpm) and (b) total Greek winter precipitation (anomalies in mm; contour interval 10 mm). They explain 16% (500 hPa geopotential height) and 14% (Greek precipitation) of the total variance. Solid lines mark the positive values and dashed lines the negative values. (c) Normalized time components of the second CCA patterns of geopotential height anomalies (dashed line) and Greek precipitation anomalies (solid line). For clearness, the monthly (DJF) time components were averaged to 1 seasonal winter value for the respective years. The correlation between the 2 seasonal curves is 0.58

#### 4.5. Synoptic situations and precipitation distribution of selected winters

Figs. 11 to 13 show the 500 hPa and precipitation anomaly fields for the winters 1962/63, 1970/71 and 1991/92. This analysis gives insight into how the most important CCA pair is associated with the atmospheric circulation and the precipitation conditions over Greece.

Fig. 11 presents the mean monthly 500 hPa geopotential height anomalies and the monthly mean precipitation anomalies (departures from the reference period 1958–1994) for the winter 1962/63 (negative time components in both data sets, cf. Fig. 8c). All months show a similar 500 hPa geopotential height anomaly distribution with negative values in an extended belt from the Atlantic over the European continent up to Russia. The centers of maximum negative departures are approximately over western and

central Europe. Positive 500 hPa geopotential height anomalies can be found east of the Black Sea and over northwestern Europe. Anomalous westerly to south-westerly airflow is associated with above-normal precipitation over the whole of Greece, especially in the eastern (December) and western (February) part of the country. More specifically, the anomaly precipitation patterns for January and February 1963 clearly indicate that the winter precipitation is associated with the passage of depressions along the Mediterranean and over Greece from west to east (Maheras 1982a, Kotinis-Zambakas et al. 1992). The primary effect of the mountains (central mountain area and Pindos chain) in the western part of the country is to promote convection by destabilizing the air upstream leading to the pronounced luv/lee effects even on a monthly or seasonal basis.

The 1970/71 winter 500 hPa geopotential height anomalies and the precipitation anomalies over

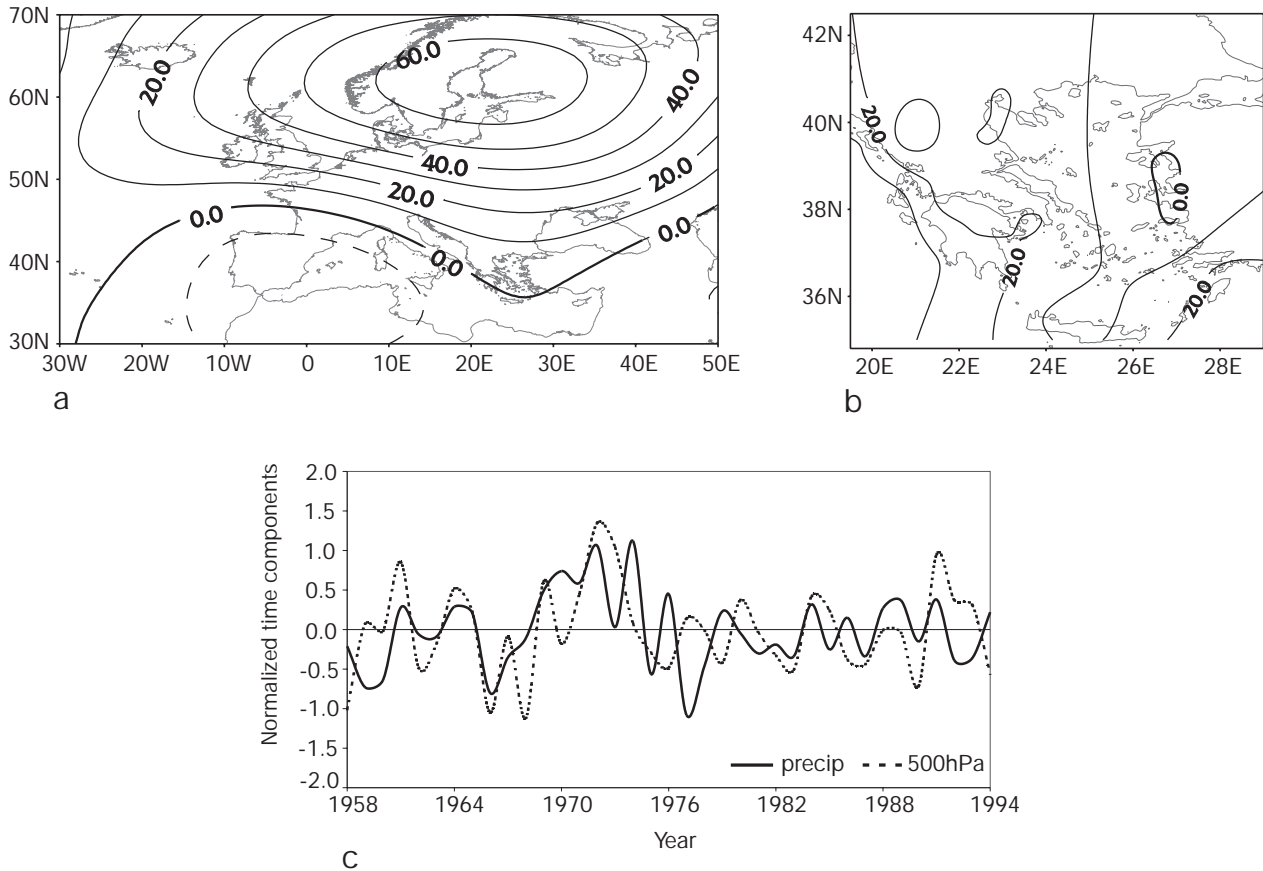


Fig. 10. Patterns of the third canonical pair of (a) winter 500 hPa geopotential height (anomalies in gpm; contour interval 10 gpm) and (b) total Greek winter precipitation (anomalies in mm; contour interval 10 mm). They explain 17% (500 hPa geopotential height) and 13% (Greek precipitation) of the total variance. Solid lines mark the positive values and dashed lines the negative values. (c) Normalized time components of the third CCA patterns of geopotential height anomalies (dashed line) and Greek precipitation anomalies (solid line). For clearness, the monthly (DJF) time components were averaged to 1 seasonal winter value for the respective years. The correlation between the 2 seasonal curves is 0.38

Greece, with time components close to zero (cf. Fig. 8c), are presented in Fig. 12. Although the averaged wintertime components indicate ‘normal’ conditions (climatology of the period 1958–1994), the 3 single winter months show a different picture, with high month-to-month variability reflected in both the anomalous mid-tropospheric circulation and the precipitation distribution. In December 1970, normal to below-normal precipitation over Greece is connected with slightly positive 500 hPa geopotential height anomalies in the vicinity of Greece and negative departures over southwestern Europe/Azores and positive departures north of around 45°N. The absolute mid-troposphere chart indeed shows a ridge from the Azores towards Iceland, a trough over France and a small ridge over the central and eastern Mediterranean (not shown).

January 1971 shows a dipole pattern with above-normal 500 hPa geopotential heights east of around

20°E and below-normal values west from central Europe, connected with a trough over the central and eastern Mediterranean in the absolute charts (not shown). The anomaly chart indicates a generally southerly upper level flow over Greece, which brings normal precipitation totals over almost the whole country. The map for February 1971 gives the reverse anomaly 500 hPa geopotential height distribution compared to January 1971, connected with above-normal precipitation values over the whole of Greece. The maximum is reached in the Ionian Sea and over the southern Aegean Sea. The absolute 500 hPa geopotential height chart for February 1971 reveals a north-westerly mid-tropospheric flow over Greece (not shown).

Similar to the previous figures, Fig. 13 shows the monthly 500 hPa geopotential height anomalies and the connected precipitation anomalies for the winter 1991/92. This winter was characterized by the most

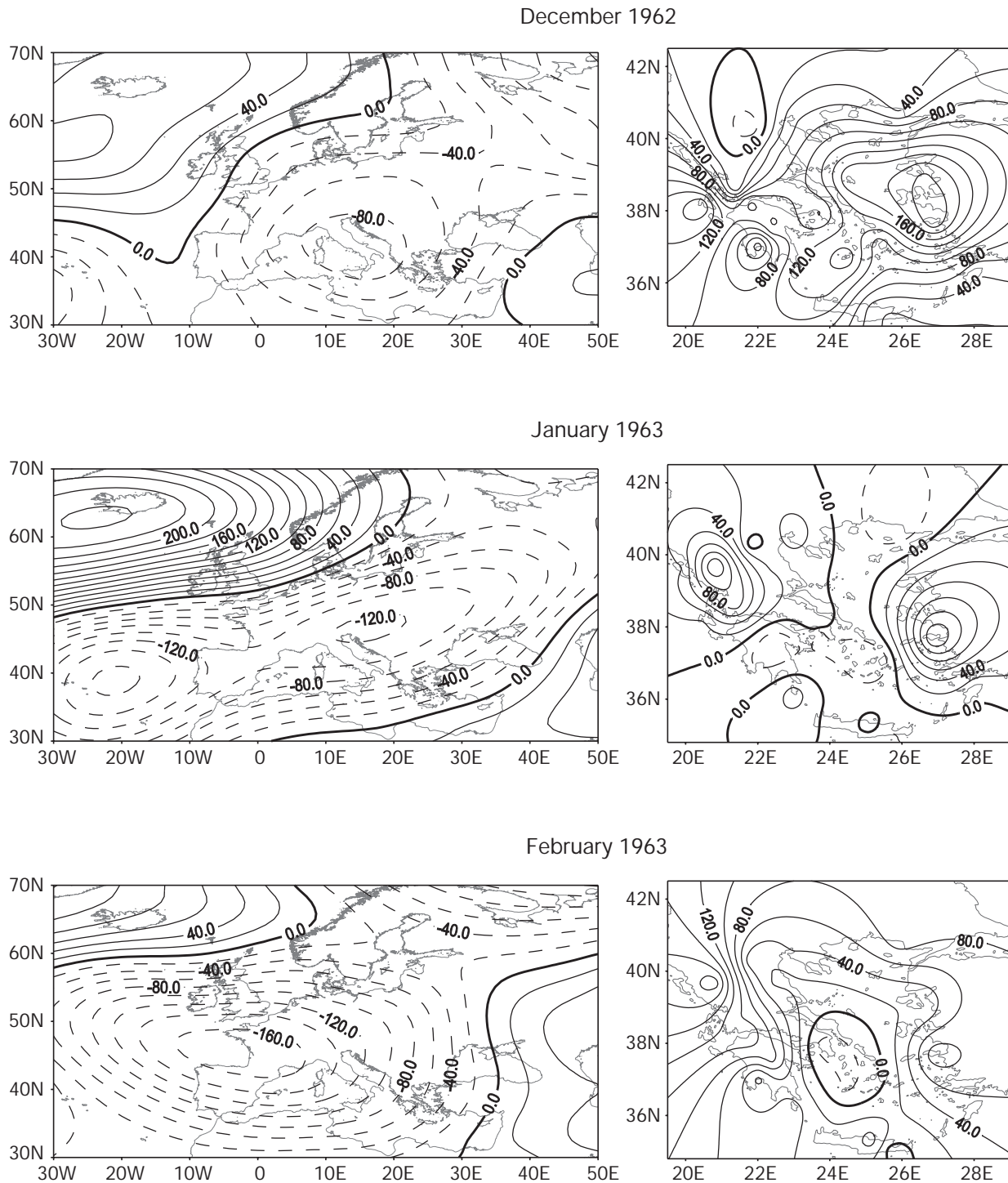


Fig. 11. Monthly mean 500 hPa geopotential height anomalies (gpm) (left) and precipitation anomalies (mm) (right) (departures from the reference period 1958–1994) for winter 1962/63 (DJF) (contour intervals are 20 gpm and 20 mm, respectively). Solid lines mark the positive values and dashed lines the negative values. This winter is representative of negative normalized time components of both Greek precipitation and 500 hPa geopotential height in the first CCA

positive normalized time components for the first CCA pair, which correlates with dryness over Greece. The monthly 500 hPa geopotential height anomalies for this

winter clearly indicate positive departures over wide parts of Europe. The center of the positive anomaly lies over northwestern Europe (British Isles) with values up

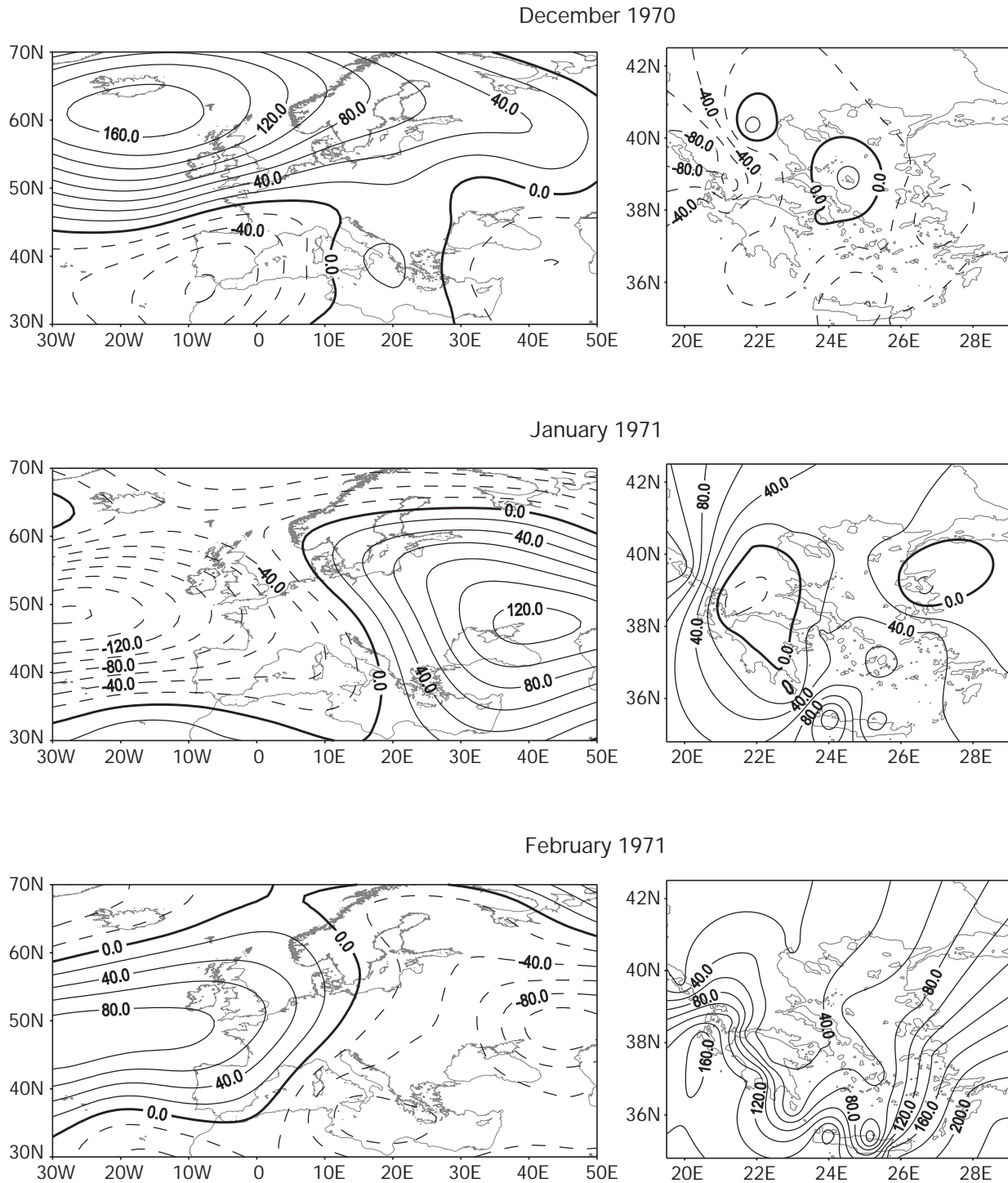


Fig. 12. Monthly mean 500 hPa geopotential height anomalies (gpm) (left) and precipitation anomalies (mm) (right) (departures from the reference period 1958–1994) for winter 1970/71 (DJF) (contour intervals are 20 gpm and 20 mm, respectively). Solid lines mark the positive values and dashed lines the negative values. This winter is representative of normalized time components close to zero of both Greek precipitation and 500 hPa geopotential height in the first CCA

to 220 gpm higher than the long-term mean. Greece is located at the southeastern part (January and February 1992) of the strong positive anomaly connected with

postfrontal subsidence and drier air. In January and February, dry and cold air is advected from the northwest (not shown), leading to distinctly below-normal precip-



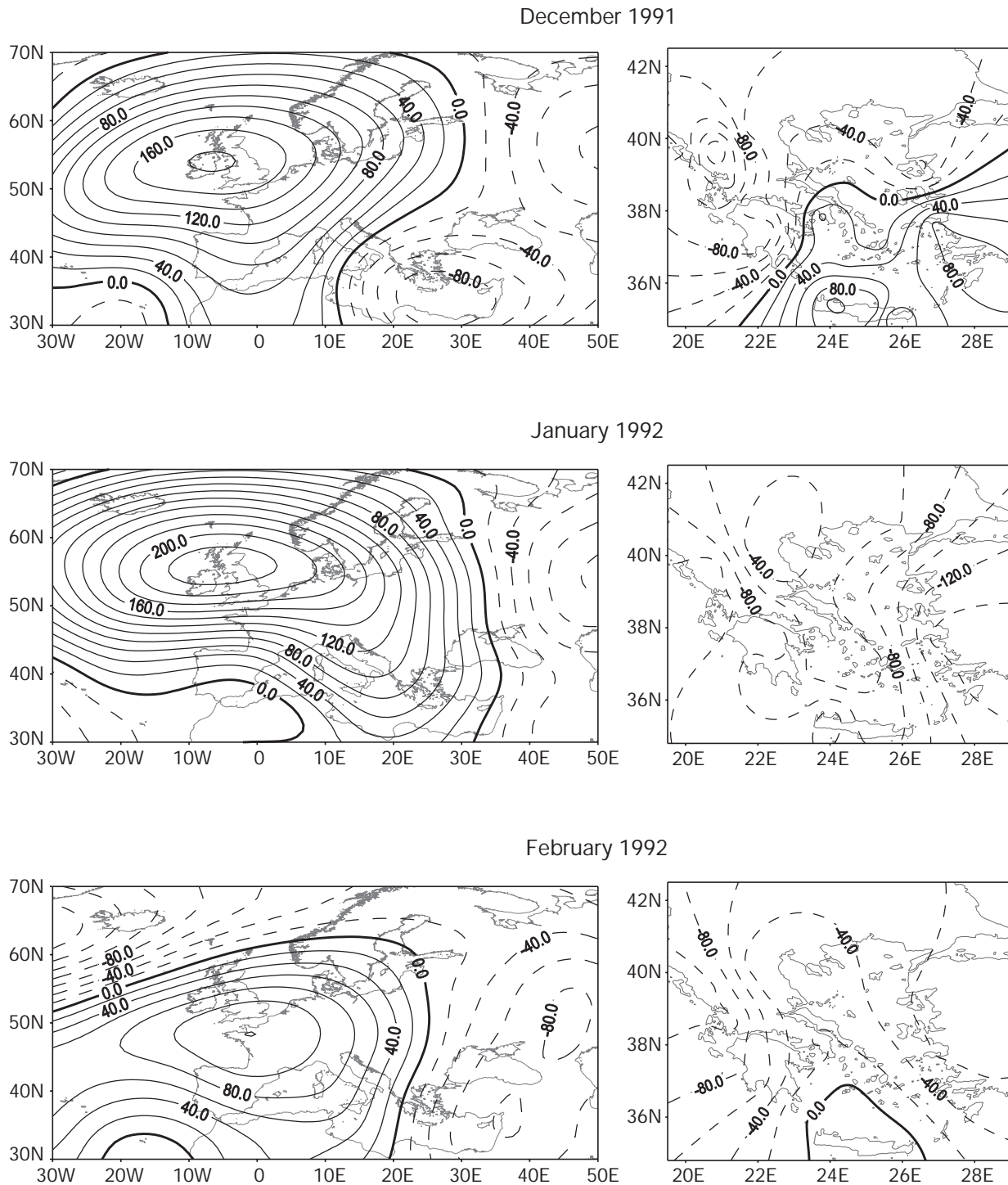


Fig. 13. Monthly mean 500 hPa geopotential height anomalies (gpm) (left) and precipitation anomalies (mm) (right) (departures from the reference period 1958–1994) for winter 1991/92 (DJF) (contour intervals are 20 gpm and 20 mm, respectively). Solid lines mark the positive values and dashed lines the negative values. This winter is representative of positive normalized time components of both Greek precipitation and 500 hPa geopotential height in the first CCA

itation over the whole of Greece. For December 1991 negative 500 hPa geopotential height anomalies were prevalent over southeastern Europe, in connection with

a mid-tropospheric trough (not shown) with above-normal precipitation totals over southern Greece and dryness over the northern part of the country.

## 5. DISCUSSION

The Mann-Kendall trend test reveals a downward trend in winter precipitation in Greece and supports the findings of Schönwiese et al. (1994, 1998). However, the denser station network reveals that only the northern and eastern parts of the country show a significant trend.

Climate models simulating the greenhouse-gas (GHG)-induced global climate trends (Houghton et al. 1990, 1992) are very restricted in their regional reliability. Nevertheless, some indications from climate modeling that GHG forcing may be responsible for the winter dryness in the Mediterranean area exist (Houghton et al. 1990, 1992).

Discussions of possible causes of the observed precipitation trends during the last decades are very complicated and problematic. Precipitation anomalies are more influenced by smaller time scale processes than temperature anomalies, resulting in a dispersed and less coherent pattern. Consequently, the CCA patterns for precipitation share less variance and are, therefore, more complicated than those related to temperature (not shown); this has also recently been stated by Corte-Real et al. (1995).

Maheras et al. (1999b) investigated wet and dry monthly anomalies across the Mediterranean Basin and their relationship with circulation over the last 130 yr. They found that the reduction in the winter precipitation can be attributed to the enhanced frequency of zonal circulation over the Mediterranean, whereas the reduction in winter temperature and winter precipitation over the Greek area can be attributed to the enhanced frequency of the northwest or northeast continental, dry and cold airflow over Greece (Maheras et al. 1999a,b). The advection of continental air is connected with the presence of high-pressure systems located over the Balkans, eastern or western Europe. The winter geopotential height fields in Fig. 13 support these results. In addition, Wanner et al. (1997) and Schönwiese et al. (1998) found for the last few decades a statistically significant upward trend in the surface pressure and the geopotential height over the eastern Atlantic and most of continental Europe, including Greece. This is due to the strengthening of the south-westerly jet over the North Atlantic area; central Europe lies to the southeast in the right exit zone of this jet. This leads to an ageostrophic cross-isobar, northwest-southeast mass transport and therefore a rise in pressure in the lower troposphere, due to imbalance of the flow in the northeastern diffluent zone of this jet (Ryd-Scherhag divergence theory; Scherhag 1948, 1952, Wanner et al. 1997). In addition, the continental flow component out of Africa has strengthened over the western part of the Mediterranean, whereas over

its eastern parts the northeasterly flow component has increased (Malberg & Frattesi 1995).

The patterns of the first CCA pair (Fig. 8a,b) and the corresponding normalized time components reflect this situation and represent a link that is very reasonable from a physical point of view: in winters with positive normalized time components, strong positive geopotential height anomalies prevail over Europe, whereas negative anomalies are dominant over the eastern North Atlantic and the eastern Mediterranean extending northward to Russia. Anomalous mid-tropospheric northerly to northeasterly air currents from northern Europe and western Russia, driven by the high, are connected with a lack of precipitation over the Greek area (see also Fig. 13). Subsidence within the anticyclone contributes to the stabilization of the air mass in the first approximately 5.5 km; thus heat exchange is restricted to the layers below the ground inversion. Analogously, opposite synoptic processes with reversed climate behavior take place with negative normalized time components. The patterns are similar with the second CCA pair provided by Corte-Real et al. (1995) connected with a Mediterranean Oscillation bringing wetter (positive normalized time components) conditions over the Iberian Peninsula, Egypt and the Near East.

The patterns of the second CCA pair (Fig. 9a,b) resemble the first CCA pair by Corte-Real et al. (1995) and represent also a reasonable link considering the overlying physics: due to subsidence and stability conditions, driven by the anomalous high geopotential heights from the eastern Mediterranean to western Russia, negative precipitation anomalies cover most of the Greek area. This is in agreement with the study of Wibig (1999), who found a similar precipitation distribution related to the Eurasian pattern (EU2; Barnston & Livezey 1987).

The concomitant patterns of the third CCA pair (Fig. 10a,b) represent a physical plausible link as well: higher (lower) than normal precipitation over the western and southeastern (north, eastern and central) part of Greece is evident in the associated precipitation pattern. The higher precipitation totals over western Greece and the Ionian Sea islands might result from anomalous southeasterly flow at the eastern flank of the upper level trough. In the opposite phase, the negative geopotential height anomalies far to the north and the positive anomalies over the western Mediterranean lead to a lack of precipitation over western Greece due to atmospheric stability (Maheras 1982a,b). Wibig (1999) found a similar precipitation distribution related to the Scandinavian pattern (Scand; Barnston & Livezey 1987, Rogers 1990).

No notable changes were found in the CCA analyses when using the first EOFs accounting for 85 and 90%

of total winter 500 hPa geopotential height variance for the subsequent CCA analysis, which is an indication that the results are not sensitive to different EOF truncations. In addition, the previous study of Xoplaki et al. (1998) revealed similar results when using a smaller  $5^\circ \times 5^\circ$  resolution of the 500 hPa geopotential height fields (30 to  $65^\circ$  N,  $20^\circ$  W to  $40^\circ$  E).

The anomalous dryness over the eastern Mediterranean and the exceptionally wet conditions over Scandinavia and northern Europe during the last years or even decades are strongly associated to the recent behavior of the North Atlantic Oscillation (NAO) (Hurrell 1995, 1996). Hurrell (1995) points to the fact that the recent, decade-long low totals of winter precipitation over the whole Mediterranean are related to the persistent positive mode of the NAO. The changes in the mean circulation patterns over the North Atlantic are also accompanied by a pronounced shift in the storm tracks and associated synoptic eddy activity as well as the transport of atmospheric moisture (Hurrell 1995, Halpert & Bell 1997). The positive NAO situation over the middle latitudes led to a maximum moisture transport from the Atlantic towards northern Europe, whereas a reduction of the total atmospheric moisture transport occurred over southern Europe and the eastern Mediterranean.

The approximately equivalent barotropic structure of the atmosphere in the first SLP (Luterbacher et al. 1998) and 500 hPa geopotential height CCA patterns does not only lead to lack of precipitation over Greece but also to below-normal winter temperatures at the surface and up to about the 850 hPa level (Proedrou et al. 1997, Luterbacher et al. 1998). Different studies have reported a tropospheric warming widespread over Europe connected with a stabilization between different layers in the troposphere (Meyrhöfer et al. 1996, Born & Flohn 1997, Maheras et al. 1998, Schönwiese et al. 1998), and thus reduced baroclinic conditions. It is worth mentioning that enhanced westerlies over the eastern North Atlantic are also linked to SST changes in the North Atlantic. Between 1973 and 1992 the SSTs of both the southern and eastern North Atlantic raised around  $1^\circ\text{C}$ . In contrast, during positive modes of the NAO, negative SST anomalies occur in the whole Mediterranean Sea (Rogers & van Loon 1979). This is in agreement with the results of Bartzokas et al. (1994), who found a marked decrease in the winter SSTs in the eastern part of the Mediterranean, with a minimum in the 1970s. The combination of subsidence in all levels together with smaller capacity for retaining precipitable water vapor due to negative SST anomalies in combination with below-normal surface temperature might lead to less sensible and latent heat flux into the lower atmosphere, and thus less precipitation.

Much more work has to be done in the future taking into consideration not only statistical analysis but also conceptual models explaining the main physics, mechanisms and processes. Further studies will investigate the large-scale atmospheric circulation patterns at the surface and in the mid-troposphere over the eastern North Atlantic European area coupled with Greek precipitation and temperature for the other seasons, both concurrently and with time-lags, which may be helpful for long-range forecasts. Further investigations of general circulation models (GCMs) with respect to simulating regional precipitation over Greece connected with SLP and the 500 hPa geopotential height fields will be conducted.

## 6. CONCLUSIONS

The influence of the large-scale mid-tropospheric circulation for wintertime on the Greek precipitation anomalies was investigated.

The Alexandersson test revealed that the Greek station precipitation data can be considered homogeneous.

The Mann-Kendall trend test indicated a significant decrease of winter precipitation in the western mountainous regions, over northern and eastern Greece from 1958 to 1994. The other regions showed reduced, although not significant, precipitation.

The 3 most important 500 hPa geopotential circulation regimes concurrently correlated with precipitation anomalies over the Greek area are plausible from the physical point of view. The links are strong and it can be asserted that changes in the Greek precipitation conditions are due to changes in the large-scale atmospheric circulation, primarily related to the first and second EOFs of 500 hPa geopotential height, i.e., to enhanced westerlies over the eastern North Atlantic, connected with a rise of the mid-tropospheric geopotential over most of continental Europe.

More wintertime blocking situations over the last 30 yr or so and thus reduced frequency of depression activity over the whole Mediterranean area led to anomalous cold and dry air advection from northerly directions towards southeastern Europe.

It is supposed that the decrease of cyclonic situations over Europe during the last few decades together with a stronger continental flow component at the surface and in the mid-troposphere was the main reason for the dry winters over Greece. In addition, negative SST anomalies in the central and eastern Mediterranean combined with reduced surface temperatures led to enhanced stabilization in the lower atmosphere.

However, climatic research is still far away from being able to explain all the different links between

the atmosphere, ocean, sea-ice, biosphere, etc., particularly in respect to all regional peculiarities (Schönwiese et al. 1994).

**Acknowledgements.** The authors wish to thank Prof. Hans von Storch (GKSS, Geesthacht), Prof. Heinz Wanner, Dr Ralph Rickli and Dr Dimitrios Gyalistras (University of Bern) for many suggestions on a former version of this paper and fruitful discussions. Christoph Schmutz (University of Bern) is acknowledged for his statistical advice and the Mann-Kendall test program, and Dr Christoph Beck (University of Würzburg) for advice concerning the homogenization procedure. Thanks are also due to Nicolas Schneider (University of Bern) for drawing the topography chart of Greece and the NCEP/NCAR for providing the reanalysis data. We are grateful to the 2 anonymous reviewers for their valuable critiques and suggestions, which improved the manuscript. This research was partly supported by EU project ACCORD under contract ENV4-CT97-0530.

#### LITERATURE CITED

- Alexandersson H (1986) A homogeneity test applied to precipitation data. *J Climatol* 6:661–675
- Alpert P, Neeman BU, Shay-El Y (1990) Intermonthly variability of cyclone tracks in the Mediterranean. *J Clim* 3 (12):1474–1487
- Barnett T, Preisendorfer R (1987) Origin and levels of monthly and seasonal forecast skill for United States surface air temperatures determined by canonical correlation analysis. *Mon Weather Rev* 115:1825–1850
- Barnston AG, Livezey RE (1987) Classification, seasonality and persistence of low frequency atmospheric circulation patterns. *Mon Weather Rev* 115:1083–1126
- Bartzikas A, Metaxas DA, Ganas IS (1994) Spatial and temporal sea-surface temperature covariances in the Mediterranean. *Int J Climatol* 14:201–213
- Born K, Flohn H (1997) The detection of changes in baroclinicity and synoptic activity on the Northern Hemisphere for the period 1967–94 using two data sets. *Meteorol Z NF* 6: 51–59
- Brown TJ, Eischeid JK (1992) An examination of spatial statistical techniques for interpolation of gridded climate data. In: *Am Meteorol Soc and Environment Canada (eds) Joint Proc 12th Conf Prob Stat Atmos Sci and 5th Int Meeting Stat Climatol*, Toronto, p 739–742
- Busuioac A, von Storch H (1996) Changes in the winter precipitation in Romania and its relation to the large scale circulation. *Tellus* 48A:538–552
- Conte M, Giuffrida S, Tedesco S (1989) The Mediterranean Oscillation: impact on precipitation and hydrology in Italy. In: *Proceedings of Conference on Climate and Water, Vol 1. Publ of Academy of Finland, Helsinki*, p 121–137
- Corte-Real J, Zhang X, Wang X (1995) Large-scale circulation regimes and surface climatic anomalies over the Mediterranean. *Int J Climatol* 15:1135–1150
- Flocas AA, Giles BD (1991) Distribution and intensity of frontal rainfall over Greece. *Int J Climatol* 11:429–442
- Flocas AA, Karacostas TS (1996) Cyclogenesis over the Aegean Sea: identifications and synoptic categories. *Meteorol Appl* 3:53–61
- Fotiadi AK, Metaxas DA, Bartzikas A (1999) A statistical study of precipitation in northwest Greece. *Int J Climatol* 19:1221–1232
- Halpert MS, Bell GD (1997) Climate assessment for 1996. *Bull Am Meteorol Soc* 78:1–48
- Houghton JT, Jenkins GJ, Ephraums JJ (eds) (1990) *Climate change: the IPCC scientific assessment*. Cambridge University Press, Cambridge
- Houghton JT, Jenkins GJ, Ephraums JJ (eds) (1992) *Climate change: the IPCC scientific assessment. 1992 supplementary report*. Cambridge University Press, Cambridge
- Hurrell JW (1995) Decadal trends in the North Atlantic Oscillation: regional temperatures and precipitation. *Science* 269:676–679
- Hurrell JW (1996) Influence of variations in extratropical wintertime teleconnections on Northern Hemisphere temperature. *Geophys Res Lett* 23:665–668
- Kalnay E, Kanamitsu M, Kistler R, Collins W, Deaven D, Gandin L, Iredell M, Saha S, White G, Woollen J, Zhu Y, Leetmaa A, Reynolds R, Chelliah M, Ebisuzaki W, Higgins W, Janowiak J, Mo KC, Ropelewski C, Wang J, Jenne R, Joseph D (1996) The NCEP/NCAR 40-Year Reanalysis Project. *Bull Am Meteorol Soc* 77:437–471
- Kotinis-Zambakas SJ, Nikolakis DJ, Kandilis PJ (1992) Orographic precipitation in Greece. *Riv Meteorol Aeronaut* 52:41–46
- Kozuchowski K, Wibig J, Maheras P (1992) Connections between air temperature and precipitation and the geopotential height of the 500 hPa level in a meridional cross-section in Europe. *Int J Climatol* 12:343–352
- Lau NC (1988) Variability of the observed midlatitude storm tracks in relation to low-frequency changes in the circulation pattern. *J Atmos Sci* 45:2718–2743
- Lolis CJ, Bartzikas A, Metaxas DA (1999) Spatial covariability of the climatic parameters in the Greek area. *Int J Climatol* 19:185–196
- Luterbacher J, Xoplaki E, Maheras P (1998) Large-scale atmospheric circulation patterns connected with winter rainfall over Greece. In: *Proceedings of 5th Greek National Congress on Meteorology-Climatology and Physics of the Atmosphere, Athens, Greece, September 1998. National Meteorological Service, Athens*, p 85–92
- Lycoudis S, Proedrou M, Kontoyannidis S, Tselepidaki L (1994) Study on the trends of precipitation, for various precipitation regimes, over Northern Greece. In: *Proceedings of 2nd Greek National Congress Meteorology-Climatology and Physics of the Atmosphere, Thessaloniki, Greece. Meteorological Climatological Institute of Thessaloniki, Thessaloniki*, p 359–368
- Maheras P (1982a) *Climatologie de la mer Egée et de ces marges continentales. Etude de climatologie descriptive et de climatologie dynamique. Thèse d'Etat, Atelier de Reproduction de Thèses de Lille III*
- Maheras P (1982b) Synoptic conditions and multi-dimensional analysis of weather in Thessaloniki. *Monograph No. 15, Publ Lab Climatology, University of Athens*
- Maheras P, Kolyva-Machera F (1979) Les espaces et les régimes pluviométriques dans la mer Egée. *Bull Hellen Meteorol Soc* 4:1–17
- Maheras P, Kolyva-Machera F (1993) Drought and its dynamic causes over the Greek area. In: *Proceedings of 3rd Greek National Geographical Congress. Thessaloniki, Greece. Hellenic Geographical Society, Athens*, p 529–546
- Maheras P, Kutiel H, Patrikas I, Kolyva-Machera F (1998) Spatial and temporal trends in 850, 700 and 500 hPa, air temperatures, over Europe and the Mediterranean during the 1962–1994 period. In: *Proceedings of 5th Greek National Congress on Meteorology-Climatology and Physics of the Atmosphere, Athens, Greece, September 1998. National Meteorological Service, Athens*, p 285–290



- Maheras P, Xoplaki E, Davies TD, Martin-Vide J, Barriendos M, Alcoforado MJ (1999a) Warm and cold monthly anomalies across the Mediterranean basin and their relationship with circulation; 1860–1990. *Int J Climatol* 19:1697–1715
- Maheras P, Xoplaki E, Kutiel H (1999b) Wet and dry monthly anomalies across the Mediterranean basin and their relationship with circulation, 1860–1990. *Theor Appl Climatol* 64:189–199
- Malberg H, Frattesi G (1995) Changes of the North Atlantic sea surface temperature related to the atmospheric circulation in the period 1973 to 1992. *Meteorol Z NF* 4:37–42
- Metaxas AD (1978) Evidence on the importance of diabatic heating as a divergence factor in the Mediterranean. *Arch Met Geophys Biokl Ser A* 27:69–80
- Metaxas AD, Kallos G (1980) High rainfall amounts over Greek Mainland during December and January. In: *Proceedings of First Hellenic-British Climatological Meeting*, Athens, Greece. National Meteorological Society, Athens, p 1–17
- Metaxas AD, Bartzokas A, Repapis CC, Dalezios NR (1993) Atmospheric circulation anomalies in dry and wet winters in Greece. *Meteorol Z NF* 2:127–131
- Meyrhofer S, Rapp J, Schönwiese CD (1996) Observed three-dimensional climate trends in Europe, 1961–1990. *Meteorol Z NF* 6:90–94
- Papadopoulos A (1993) Dentrechronologie du pin d'Alep en Grèce; Contribution aux études climatologiques. *Publ de l'Association Internationale de Climatologie (AIC)* 6:253–262
- Peterson TC, Easterling DR, Karl TR, Groisman P, Nicholls N, Plummer N, Torok S, Auer I, Boehm R, Gullett D, Vincent L, Heino R, Tuomenvirta H, Mestre O, Szentimrey T, Salinger J, Førland EJ, Hanssen-Bauer I, Alexandersson H, Jones P, Parker D (1998) Homogeneity adjustments of in situ atmospheric climate data: a review. *Int J Climatol* 18:1493–1517
- Preisendorfer RW (1988) Principal component analysis in meteorology and oceanography. *Developments in atmospheric sciences*, Vol 17. Elsevier, Amsterdam, p 293–318
- Prezerakos NG, Flocas HA (1996) The formation of a dynamically unstable ridge at 500 hPa in northwest Europe as a precursor of surface cyclogenesis in central Mediterranean. *Meteorol Appl* 3:101–111
- Prezerakos NG, Flocas HA (1997) The role of a developing upper diffluent trough in surface cyclogenesis over central Mediterranean. *Meteorol Z NF* 6:108–119
- Proedrou M, Theoharatos G, Cartalis C (1997) Variations and trends in annual and seasonal air temperature in Greece determined from ground and satellite measurements. *Theor Appl Climatol* 10:401–405
- Repapis C, Amanatidis G, Paliatatos A, Mantis H (1993) Cohérence spatiale des précipitations en Grèce. *Publ de l'AIC* 6:333–340
- Rizou C, Karacostas T (1993) Etude des précipitations engendrées par les systèmes dépressionnaires d'origine SW sur le territoire Hellénique. *Publ de l'AIC* 6:351–361
- Rogers JC (1990) Patterns of low-frequency monthly sea level pressure variability (1899–1986) and associated wave cyclone frequencies. *J Clim* 3:1364–1379
- Rogers JC, van Loon H (1979) The seesaw in winter temperatures between Greenland and northern Europe. Part II: Some oceanic and atmospheric effects in Middle and High latitudes. *Mon Weather Rev* 107:509–519
- Sahsamanoglou H (1993) Etude des précipitations dans les Balkans basée sur l'analyse en composantes principales. *Publ de l'AIC* 6:291–300
- Sakellariou N, Papadopoulos A, Kambezidis H, Psiloglou B, Assimakopoulos D (1993) Analyse de corrélations des pluies mensuelles au niveau des stations de la mer Egée. *Publ de l'AIC* 6:285–290
- Scherhag R (1948) *Wetteranalyse und Wetterprognose*. Springer, Heidelberg
- Scherhag R (1952) Die explosionsartigen Stratosphärenwärmungen des Spätwinters 1952. *Ber Dtsch Wetterd US-Zone* 38:51–63
- Schönwiese CD, Rapp J, Fuchs T, Denhard M (1994) Observed climate trends in Europe 1891–1990. *Meteorol Z NF* 3:22–28
- Schönwiese CD, Walter A, Rapp J, Meyhöfer S, Denhard M (1998) Statistische Analyse der Klimavariabilität und anthropogenen Klimasignale in globaler und regionaler Betrachtung. *Ber Inst Meteor und Geophys Univers Frankfurt/Main*, Nr 102, Eigenverlag des Instituts, Frankfurt/Main
- Sneyers R (1992) On the statistical analysis of series of observations. *WMO Publ No.* 415 (Tech Note No. 143), Geneva
- Trenberth KE (1990) Recent observed interdecadal climate changes in the Northern Hemisphere. *Bull Am Meteorol Soc* 71:989–993
- Trigo IF, Davies TD, Bigg GR (1999) Objective climatology of cyclones in the Mediterranean Region. *J Clim* 16:1685–1696
- von Storch H (1995) Spatial patterns: EOFs and CCA. In: von Storch H, Navarra A (eds) *Analysis of climate variability: applications of statistical techniques*. Springer, Heidelberg, p 227–258
- von Storch H, Zwiers FW (1999) *Statistical analysis in climate research*. Cambridge University Press, Cambridge
- Wanner H, Rickli R, Salvisberg E, Schmutz C, Schüepp M (1997) Global climate change and variability and its influence on alpine climate—concepts and observations. *Theor Appl Climatol* 58:221–243
- Wibig J (1999) Precipitation in Europe in relation to circulation patterns at the 500 hPa level. *Int J Climatol* 19:253–269
- Xoplaki E, Luterbacher J, Patrikas J, Maheras P (1998) Les précipitations hivernales en Grèce et leurs relations avec la circulation atmosphérique à grande échelle au niveau de 500 hPa. *Publ de l'AIC* 11:374–382
- Xoplaki E, Luterbacher J, Burkard R (1999) Influence of large scale atmospheric circulation on the variability of seasonal precipitation in Thessaloniki, 1958–1997. In: Special edition to mark the 70th year since the establishment of the Dept of Meteorology and Climatology of Aristotelian University of Thessaloniki. *Meteorological Climatological Institute of Thessaloniki*, Thessaloniki, p 93–102 (in Greek)
- Xu JS (1993) The joint modes of the coupled atmosphere-ocean system observed from 1967 to 1987. *J Clim* 6:816–838
- Yarnal BM, Diaz HF (1986) Relationship between extremes of the Southern Oscillation and the winter climate of the Angloamerican Pacific coast. *J Climatol* 6:197–219